Recovery of noble metal elements from effluents of the semiconductor industry as nanoparticles, by dielectric barrier discharge (DBD) plasma treatment

Jean-François Sauvageau[a,b,c], Marc-André Fortin[a,b,c,*]

[a] *Département de Génie des Mines, de la Métallurgie et des Matériaux, Université Laval, Québec G1V 0A6, Canada.*
[b] *Axe Médecine Régénératrice, Centre Hospitalier Universitaire (CHU) de Québec, 10 rue de l'Espinay, Québec G1L 3L5, Canada.*
[c] *Centre de recherche sur les matériaux avancés (CERMA), Université Laval, Québec G1V 0A6, Canada.*

* Corresponding author.
E-mail address: marc-andre.fortin@gmn.ulaval.ca

Keywords: Plasma, Nanoparticles, Electroless plating, Effluents

(***Published in Hydrometallurgy (Elsevier); accepted September 15, 2020)

Abstract

The fabrication of semiconductor products for the microelectronic industry requires the deposition of thin noble metal layers (e.g. Au-Sn and Pd) by means of processes involving fluid baths that contain metal ions (e.g. electrowinning and electroless plating). After several cycles, the plating solutions are used up and must be replaced, generating large volumes of discarded solutions containing precious metals. The metals (Au and Pd) are recovered either by electrowinning, a slow batch process, or by the use of toxic molecules (e.g. cyanides). This study demonstrates the possibility of using an atmospheric plasma technology to recover Au and Pd from these solutions, which provides a faster and greener process. Plasma discharges are generated at the surface of the solutions, causing ions to precipitate as nanoparticles. The treatment (few minutes only) allows the recovery of >95% gold, and >60% palladium. The process separates Au (NPs) from Sn ions (remaining in solution), as confirmed by elemental analysis and XPS. Particle size distributions of the nanoparticles recovered through the process suggests that as-

synthesized nanoparticles could integrate value-added products (e.g. catalyst industry). Overall, the use of plasma technology could open several possibilities for the recycling of metals contained in solutions discarded from the semiconductor industry.

1 Introduction

The fabrication of several semiconductor products in the electronic industry requires the deposition of a variety of metal layers on flat semiconductor surfaces.(Azmah Hanim, 2017) This is usually achieved by means of precisely tuned electrochemical-based processes. Among the most frequent metal thin films deposited onto semiconductor surfaces, figure Au, Au-Sn alloys, as well as Pd.(Azmah Hanim, 2017; Datta and Osaka, 2005) As several of the plated metals are noble and costly, the electrodeposition (or electroless) processes must be efficient, with yields allowing the consumption of a large fraction of the noble elements dissolved in electrolyte solutions. Both electroplating and electroless plating require electrolyte baths containing metal ions and other additives.(Osaka et al., 2006; Statista, 2017) Metal ions are reduced onto the surface of a substrate either by the application of an electric current (electroplating) or, for electroless plating, by the use of reducing agents contained in the electrolyte baths (e.g. hydrazine, hypophosphite, benzyl alcohol).(Azmah Hanim, 2017; Osaka et al., 2006; Vorobyova et al., 2004) Electroless plating does not require electric current to reduce the metal ions; therefore, electroless plating allows the fabrication of isolated metal patterns on insulating substrates.(Azmah Hanim, 2017; Shacham-Diamand et al., 2015) On the other hand, electroless plating is associated with a more complex control over the composition of the electrolyte baths and with higher operation costs compared to electroplating.(Loto, 2016; Shacham-Diamand et al., 2015)

In both processes, the electrolyte solutions must be frequently refreshed. First, the concentration in noble metal ions must remain above a certain threshold during the process. Then, the presence of parasite, poisoning or competitive chemical species in the electrochemical baths can affect the plating process.(Shacham-Diamand et al., 2015) In fact, large volumes of liquids containing noble metals and toxic chemical species such as cyanides, must be periodically discarded by the semiconductor industry.(Azmah Hanim, 2017; Frost et al., 2017; Shacham-Diamand et al., 2015) Disposing of these large volumes of contaminated chemicals represents a real challenge for the industry. To recover the precious metal contents from the discarded solutions, the semiconductor industries mainly use electrowinning cells, which is a relatively slow batch process technology that is not very efficient at metal ion concentrations below 10 mM.(Barbosa et al., 2001) The foils or plates of recovered metals are usually contaminated by different metals in the baths, which requires further manipulations and separation processes. In addition to this, the electrolyte solutions must be treated appropriately in order to attenuate their toxicity (e.g. elimination of cyanides). Thus high costs are associated to the disposal of electrolyte waste, and recycling the precious metals from these effluents is not straightforward. In the last few years, alternative methods based on biotechnological approaches (e.g. using microbes, microalgae, etc.) have also been studied in order to recover noble metals such as Au and Pd from synthetic solutions as nanoparticles.(Ali et al., 2019; Luangpipat et al., 2011) However, further optimization of these novel recovery techniques are required prior to their application for metal-bearing wastewaters. These would certainly be restricted to the development of batch processes because of the time required for biological reactions to occur in well-controlled conditions.

This article describes a new process based on atmospheric plasma technology, allowing for the rapid extraction of precious metal ions from effluents discarded by the semiconductor industry. The

process does not use toxic chemicals such as cyanides, and it is much more rapid than electrowinning (a few minutes only even with solutions containing less than 1 mM metal ions.(Bouchard et al., 2017; Sauvageau et al., 2018) In recent years, plasma technology has entered various application fields, such as water purification, surface treatments and nanoparticles synthesis (NPs).(Bouchard et al., 2015; Brandenburg, 2017; Foster, 2017; Hijosa-Valsero et al., 2013a; Hijosa-Valsero et al., 2013b; Kim et al., 2013; Kogelschatz, 2003; Kogelschatz, 2007; Kogelschatz et al., 1999; Saito et al., 2017) Atmospheric-pressure plasma systems such as dielectric barrier discharge (DBD) reactors can treat relatively large surfaces of solids and liquids (up to tens of cm^2).(Bednar et al., 2013; Bouchard et al., 2017; Kong et al., 2011) Recent works including from our team have reported the use of plasmas to synthesize Au, Pd, Pt and Rh NPs from metal ion containing aqueous solutions, and more specifically with DBD plasma reactors.(Bouchard et al., 2017; Koo et al., 2005; Lee et al., 2013; McKenna et al., 2011; Richmonds and Sankaran, 2008; Sauvageau et al., 2018; Wang et al., 2015; Xu et al., 2012) By comparison to the conventional techniques for noble metals extraction (e.g. cyanidation, electrowinning), plasma electrochemistry could enable the rapid recovery of metals without the need to use additives, surfactants or other potentially toxic compounds.(Koo et al., 2005; McKenna et al., 2011; Sauvageau et al., 2018)

In this study, electrolyte solutions typical of the electroless plating process in the semiconductor industry for Au-Sn and Pd platings, were processed with a DBD plasma reactor (argon and hydrogen plasma). The discarded solutions, typical of those discarded from the electroless plating batch processes for Au + Sn and Pd coatings, were collected when the concentration of noble metal ions was too low to pursue the electroless plating efficiently (9.4 - 12.7 mM). After plasma treatment, the electrolyte solutions contain NPs which are separated from the residual electrolyte by centrifugation. A mass balance assessment using elemental analysis is performed to measure the ion-to-NPs conversion yield. A

physicochemical analysis study is performed with XPS to demonstrate the high metal contents of Au and Pd NPs generated by the process, as well as to identify the molecules and ions covering the surface of NPs. Finally, a particle size analysis completes the results of the study.

2 Material and methods

2.1 Chemicals and precursor solutions

Two electrolytic solutions representative of the used-up fluids discarded after several cycles of the electroless plating process, were collected and provided by an industrial partner. The first precursor solution (Au-Sn) had a gold concentration of 2.5 g L^{-1} (12.7 mM Au(I); $KAu(CN)_2$). It also contained tin (Sn(II); 42.1 mM, 5 g L^{-1}), potassium oxalate (50 – 100 g L^{-1}), as well as ascorbic acid and hydroquinone as additives in minor concentration. The second precursor solution contained Pd(II) (1 g L^{-1}; 9.4 mM in the form of palladium acetate; $Pd(O_2CCH_3)_2$), hypophosphite (a reducing agent; 15 g L^{-1}), thiourea (CH_4N_2S, a pH stabilizer), and iodine (to accelerate the metal deposition). These solutions feature components and concentrations typically found in the plating processes used in the semiconductor industry.(Azmah Hanim, 2017) Before insertion in the plasma process, the solutions were vortexed for 10 s.

2.2 Plasma treatment of Au + Sn and Pd-containing solutions

17 mL of each electrolytic solution were plasma-treated for 5 min, 10 min and 15 min. All experiments were performed in triplicate. Plasmas were generated with a mix of Ar and H_2 (95% Ar: 99.9995%, Linde Canada; 5% H_2: 99.999%, Linde Canada). The voltage and frequency used for the experiments were 15 kV peak-to-peak and 25 kHz, respectively. The power of the resulting plasma discharges was 40 W. The gas flow rate used for the syntheses was 100 mL min^{-1}, for all experiments.

To limit the formation of pulsations at the plasma-liquid interface, a peristaltic mini-pump was used to maintain the flow rate of solution at a minimum (0.5 mL s^{-1}). A detailed description of the plasma reactor that was used for this study can be found in previous works.(Bouchard et al., 2017; Sauvageau et al., 2018) The pH was measured at each step of the plasma-treatment process.

The plasma reactor used in this study features a dielectric barrier discharge (DBD).(Bouchard et al., 2017; Sauvageau et al., 2018) An AC voltage is applied between two quartz cells (48-Q-5, Spectrosil Quartz, Starna Cells) acting as cathodes and a solution containing metal ions acting as a liquid anode. The quartz cells contain cooling water, on which a sinusoidal voltage is applied. The cooling water acts as a liquid cathode and prevents overheating of the quartz cells. The cathodes and the anode are parallel, separated by a 3-mm gap and isolated from each other. A constant gas flow is introduced perpendicularly between the two electrodes. An electric field forms under the quartz cells, inducing the ionization of argon and hydrogen atoms. Thus, after the accumulation of charges at the underside of the quartz cells acting as the dielectric material, plasma microdischarges form by capacitive effect and are continuously annihilated.

The solution is first introduced in the reactor using a peristaltic pump and a silicone tubing system. All experiments in this study were performed in a closed circuit; the solutions were thus recirculated under the plasma discharges (11.25 cm^2) about 2 times min^{-1}. The process flowchart of the plasma reactor can be found in Fig. 1. Both electrolyte solutions were plasma-treated for 5, 10 and 15 min. NP nucleation and growth was rapidly revealed through a strong color change occurring in the silicone tubing. After plasma treatment, the solutions were recovered by pipetting and centrifuged to separate the synthesized NPs from the unreacted ions. A fraction of the NPs formed a coating on the walls of the plasma reactor, which was recovered with a cleaning solution of aqua regia for elemental analysis. The NPs pellet, the

supernatant and the cleaning solution were collected to perform materials characterization (NPs size measurements, elemental analysis, etc.). This methodology is described in section 2.4.

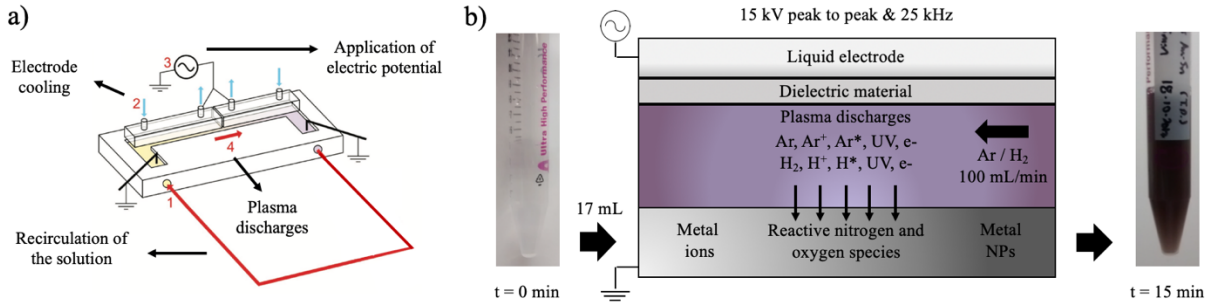

Fig. 1. a) Overview of the plasma treatment section of the plasma reactor and b) cross-sectional view of the plasma treatment area.

2.3. Separation of NPs from unreacted ions

Immediately after plasma treatment, the NPs suspensions were centrifuged at 7000 RPM for 10 min. The obtained supernatant contained the unreacted ions, while the pellet contained the NPs synthesized by plasma treatment. In previous studies performed at lower metal concentrations (1 mM Au)(Bouchard et al., 2017), we evidenced a ripening process (i.e. reduction of metal ions by chemical species generated by the plasma discharges) taking place for at least 4 hours after end of the plasma treatment. No evidence of a ripening process taking place in the supernatant solution was measured by UV-vis in the present study, and therefore the supernatant was collected by pipetting in a separate 50-mL centrifuge tube.

2.4. Digestion procedure and elemental analysis (MP-AES) of plasma-treated solutions

The metal ion – to NPs conversion yield was measured through a mass-balance assessment atomic emission spectroscopy elemental analysis. The supernatant obtained after centrifugation (mainly unreacted metal ions), as well as the NPs (pellet obtained after centrifugation) were separately digested

in aqua regia (HCl: VWR, 37%; HNO_3: VWR, 70%; aqua regia: HCl/HNO_3 = 3/1) at 80 °C. The fraction of NPs that remained on the walls of the plasma reactor after collection of the solution by pipetting, was washed in aqua regia (20 mL, 80 °C), followed by rinsing in nanopure water (20 mL, Barnstead, 18.2 MΩ). This fluid fraction was collected and measured in elemental analysis (referred to as the cleaning solution). The digested samples were analyzed by microwave plasma atomic emission spectroscopy (MP-AES 4100; improved flame and interface in the 4200 configuration). Fig. 2 summarizes the methodology that was used to prepare the samples for the mass-balance assessment by elemental analysis.

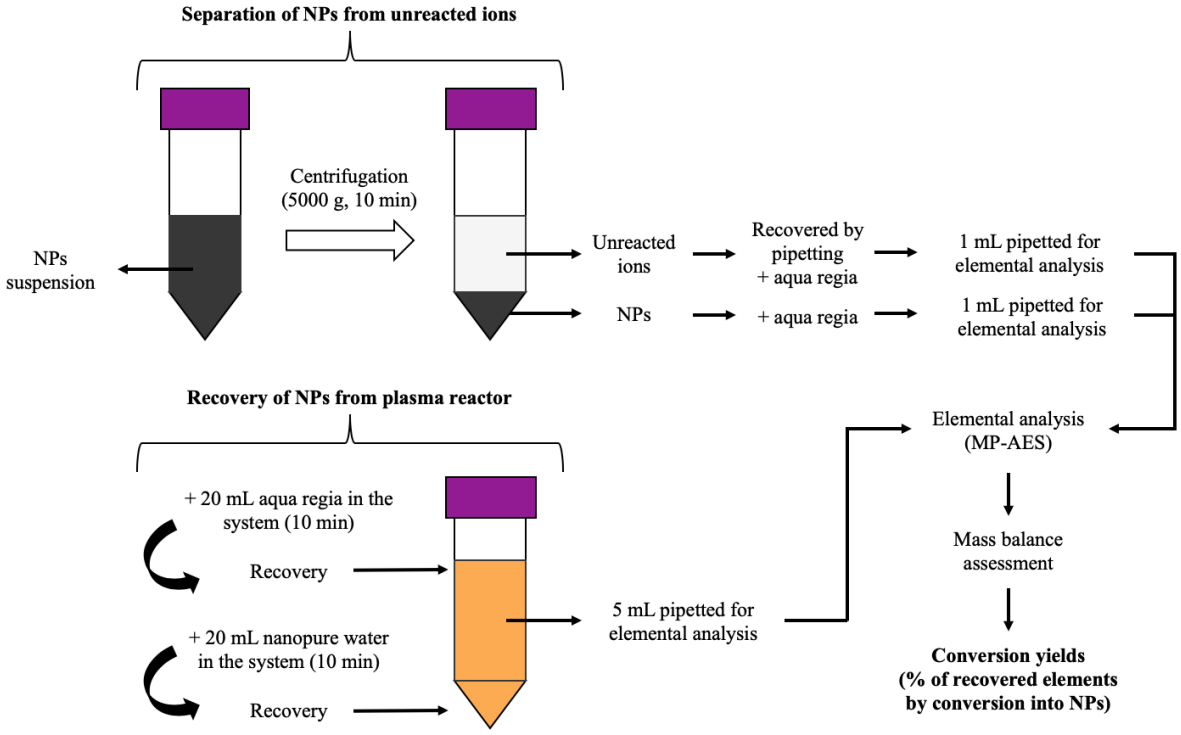

Fig. 2. Metal recovery mass-balance assessment: schematic representation for the separation of synthesized nanoparticles from unreacted ions by centrifugation, followed by digestion with aqua regia prior to MP-AES analyses.

2.5 Cleaning of the plasma reactor between the syntheses

After each synthesis, a solution of NaOH (20 mL, Sigma-Aldrich, ACS reagent, ≥ 97%, pH = 12) was recirculated in the plasma reactor in order to neutralize the remaining traces of aqua regia, followed by a few liters of nanopure water (Barnstead, 18.2 MΩ) until neutral pH was reached.

2.6 Transmission electron microscopy measurements (TEM)

After centrifugation of the plasma-treated solutions, the NPs pellet was sampled and nanopure water (2 mL, Barnstead, 18.2 MΩ) was added to the NPs. The NPs were dispersed in nanopure water using an ultrasonic bath for 10 min. 5 µL of the diluted solution were deposited on a carbon-coated copper TEM grid (300 mesh, Electron Microscopy Sciences), and imaged by TEM (120 kV, Jeol JEM-2100F, LaB_6 filament). After TEM studies, the ImageJ software was used to analyze the average diameter of the nanoparticles.

2.7 Dynamic light scattering measurements (DLS)

Prior to separation of the NPs from the unreacted ions by centrifugation, 40 µL of the plasma-treated solutions were pipetted into polystyrene micro-cuvettes to measure the hydrodynamic diameter of the synthesized NPs (Malvern Zetasizer Nano series, 173 °, 25 °C). The refractive indices of gold and palladium were set to 1.800 and 0.280, respectively.(CRC Press, 2007)

2.8 X-ray photoelectron spectroscopy (XPS)

A small fraction of the NPs pellet obtained after centrifugation was collected and nanopure water (10 mL, Barnstead, 18.2 MΩ) was added to the NPs. The NPs were dispersed in solution using an ultrasonic bath for 10 min. The NPs suspensions were then purified three times by centrifugation (7000

RPM, 20 min), the supernatants containing the impurities, additives and remaining ions, were discarded. Silicon wafers were cleaned prior to sample preparation with TL1 solution (a mixture of nanopure water (120 mL, Barnstead, 18.2 MΩ), H_2O_2 (20 mL, Fluka Analytical, ≥ 30% (RT)), and NH_4OH (20 mL, ACS reagent, 28.0 - 30.0% NH_3 basis)), followed by TL2 solution (a mixture of nanopure water (125 mL, Barnstead, 18.2 MΩ), H_2O_2 (25 mL, Fluka Analytical, ≥ 30% (RT)), and HCl (25 mL Anachemia, ACS reagent, 37%)). The wafers were then quickly rinsed with nanopure water (Barnstead, 18.2 MΩ) and anhydrous ethanol, followed by drying with medical air. The samples were prepared with NPs (20 µL) on these cleaned silicon wafers, and analyzed by XPS (PHI 5600-ci spectrometer, Physical Electronics USA). Survey scans were performed on three different regions of the silicon wafer for the sample obtained from the Au + Sn solution. However, a single survey scan was performed on the sample obtained from the Pd solution, due to a limited amount of product on the silicon wafer. High-resolution XPS scans were performed for C1s, O1s, Au4f and Pd3d peaks. An aluminum X-ray source (1486.6 eV) was used for the analyses, which were performed at 200 W for survey spectra and 150 W for high resolution spectra. Both types of analyses were performed with a detection angle of 45° relative to the surface of the samples. Atomic percentages were assessed by the Multipack software using Gaussian-Lorentzian functions for curve fitting of the peaks, after adjustment of the main C1s peak to 285.0 eV.

3. Results and discussion

Electroless plating is a surface finish deposition process widely used in semiconductor packaging. It allows for the fabrication of isolated metal patterns on insulating substrates with precise control over the thickness and quality of the deposits.(Shacham-Diamand et al., 2015) A reducing agent in the electrolyte bath (e.g. sodium hypophosphite, hydrazine, etc.) enables the chemical reduction of metal ions on the substrates without the use of electrical energy.(Azmah Hanim, 2017; Baudrand and Bengston, 1995; Shacham-Diamand et al., 2015)

3.1 Metal ion conversion and elemental analysis for mass balance assessment

The characteristics of the precursor solutions and the plasma-treated solutions, such as pH and color, can be found in Table 1. In all cases, the pH was stable at all times, regardless of the duration of the plasma treatment. This is in agreement with the nature of the buffer solutions (e.g. potassium oxalate in the Au + Sn solution). As depicted in Fig. 3, a strong color change was observed for all plasma-treated solutions, from transparent to brown for the Au-Sn solutions, and from transparent to black for the Pd(II) solutions. The quick color change of the solutions during plasma treatment was a good indication of a strong conversion of Au(I) and Pd(II) from ions into NPs. No obvious difference was noted in opacity and color from t = 5 min to t = 15 min. Temperature increase in the fluids was inferior to 5 °C in all experiments. The synthesized gold and palladium particles sedimented quickly after their synthesis, as confirmed by DLS measurements (see in supporting information Fig. S1). This is expected for as-synthesized surfactant-free metal nanoparticles.

Table 1. pH and color of the solutions before and after plasma treatment.

Solution	Duration of plasma treatment [min]	Initial pH	Final pH	Initial color	Final color
Au-Sn	5	3.5	3.5	Transparent	Brown
	10	3.5	3.5	Transparent	Brown
	15	3.5	3.5	Transparent	Brown
Pd	5	8.0	8.0	Transparent	Black
	10	8.0	8.0	Transparent	Black
	15	8.0	8.0	Transparent	Black

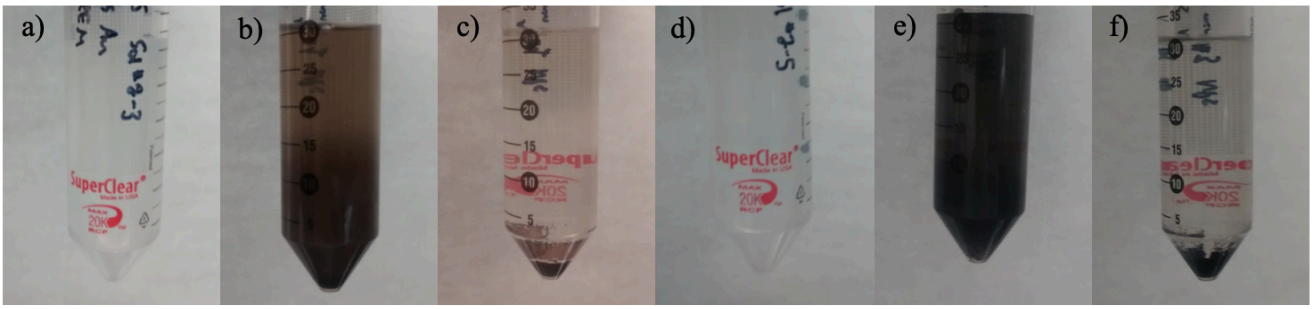

Fig. 3. a) Au-Sn precursor solution, b) Au-Sn solution plasma-treated for 15 min, c) Au-Sn NPs solution after centrifugation, d) Pd precursor solution, e) Pd solution plasma-treated for 15 min, f) Pd NPs solution after centrifugation.

3.2 Elemental analysis (MP-AES)

A mass balance assessment for the elemental recovery of gold, tin and palladium ions in the form of NPs, was calculated from the MP-AES results. The mass of metal ions initially present in the precursor solutions was compared with the mass of NPs recovered in the NPs pellet obtained after centrifugation. The small fraction of NPs remaining on the walls of the plasma reactor was recuperated by aqua regia in the cleaning solution. The method used to calculate the elemental recovery for gold, tin and palladium is summarized in Fig. 4, whereas Table 2 presents the results of the calculations performed from MP-AES data. Elemental recoveries for gold, tin and palladium can also be found in Fig. 5. Gold was recovered in a percentage ranging between 95% and 100%, without significant differences between plasma treatment times (5, 10, 15 min). In fact, after only 5 min, more than 95% of the ionic gold in solution was already converted into NPs. The only difference between the three durations of plasma treatment was the decrease of the standard deviation, from 8.90% at 5 min, to 4.31% at 10 min, and to 2.35% at 15 min. No indication of a ripening process, or further conversion of Au(I) ions into NPs after the end of plasma treatment, was found in the supernatant. Overall, these results demonstrate that plasma recovery is much more rapid than electrowinning for the recovery of Au from ionic solutions in the range 9 - 12 mM.

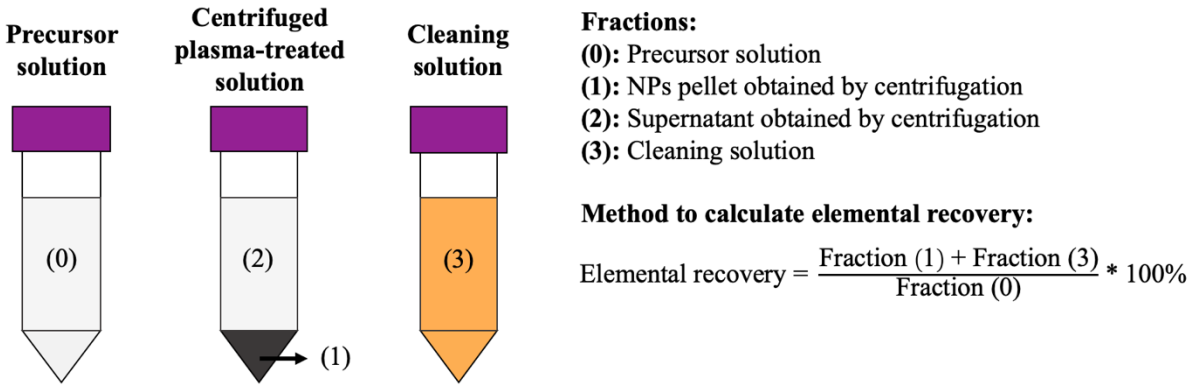

Fig. 4. Calculation method for elemental recovery of gold, tin and palladium.

Table 2. Mass fractions of gold, tin and palladium, calculated from MP-AES results (n = 3 for each duration of plasma treatment).

Element	Duration of plasma treatment [min]	Mass of ions in precursor solution [mg]	Mean recovered mass in NPs pellet [mg]	Mean recovered mass in cleaning solution [mg]	Mean mass of residual ions in supernatant [mg]	Mean elemental recovery ± standard deviation [%]
Au	5	47.82	45.18	0.54	3.00	95.6 ± 8.9
	10	47.82	47.87	0.97	1.36	102.1 ± 4.3
	15	47.82	44.41	1.58	4.36	96.2 ± 2.4
Sn	5	98.45	0.71	0.50	98.34	1.2 ± 0.2
	10	98.45	0.90	0.61	98.32	1.5 ± 0.1
	15	98.45	0.66	1.02	90.52	1.7 ± 0.4
Pd	5	15.81	5.76	0.33	6.56	38.5 ± 15.4
	10	15.81	3.84	0.97	4.90	31.0 ± 11.4
	15	15.81	5.32	1.61	3.87	43.8 ± 14.4

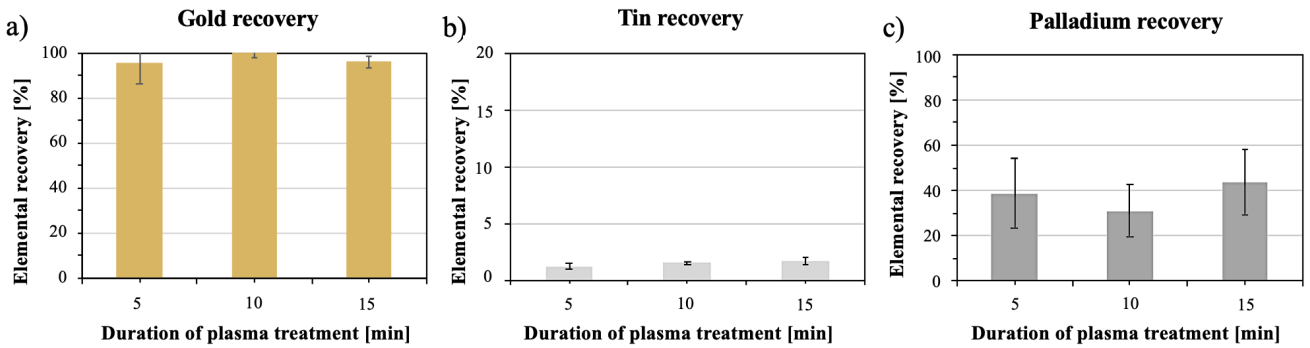

Fig. 5. Elemental recovery of a) gold, b) tin and c) palladium for the plasma-treated solutions relative to the mass of ions contained in the precursor solutions, calculated from MP-AES results (n = 3 for each duration of plasma treatment).

Very small amounts of tin were recovered in the NP pellets (< 2%) regardless of the duration of plasma treatment. Thus, Au(I) is reduced preferentially to Sn(II) and this suggests the possibility of using plasma treatment as an alternative to cyanidation to selectively extract Au from ionic solutions containing both Au and Sn. Although the exact chemical mechanisms controlling the reduction of metal ions into NPs must be studied case by case (electrolyte dependent), it is assumed that the electrochemical potential of the metal ions plays a major role in the mechanism.(Mariotti and Sankaran, 2010; Richmonds and Sankaran, 2008) The respective standard electrode potentials for the conversion of Sn^{2+} into Sn(s), and for the conversion of $Au(CN)_2^-$ into Au(s) are as follows (CRC Press, 2007):

$$Sn^{2+} + 2e^- \rightleftarrows Sn(s) \qquad E° = -0.13\ V \quad (1)$$

$$Au(CN)^{2-} + e^- \rightleftarrows Au(s) + 2CN^- \qquad E° = -0.60\ V \quad (2)$$

Although other chemical reactions are necessarily involved in the plasma process, and in particular through reactive oxygen and nitrogen species (Burlica et al., 2006; Hamaguchi, 2013; Kong et al., 2011; Mariotti and Sankaran, 2010; Nosenko et al., 2009; Yukinori et al., 2012), the large difference

between the standard electrode potentials for the two species must play a role in the very limited amount of Sn recuperated in the form of NPs. Overall, these results demonstrate for the first time that plasma electrochemistry can be used to selectively recuperate one metal ion from solutions containing many metal ion species. The fact that gold can be pre-concentrated by plasma electrochemistry could open possibilities for the replacement by plasma processes of certain metal extraction procedures involving the use of highly toxic chemicals (e.g. cyanides).

For palladium, elemental recovery yields varied from 30% to 45%, with a relatively high standard deviation (10% - 15%). No significant difference of palladium recovery was found between the durations of plasma treatment. Nonetheless, palladium recovery reached 38% after 5 min of plasma treatment and can reach up to 60% for 15 min of plasma treatment. No further evidence of NP conversion was found after 15 min of plasma treatment, suggesting that a dynamic process takes place between Pd NPs synthesis and dissolution. The nucleation rate and growth of metal nanoparticles could potentially be further increased, by generating through the plasma more reducing metastable species in solution. These would accelerate the reduction of metals ions. In addition, the continuous removal of synthesized NPs during plasma treatment in such a batch process could limit the interaction of already-synthesized NPs with reducing species, thus giving more opportunities for metal ions to be converted. Moreover, extensive characterization of the plasma discharges and its related species could lead to a more refined understanding of the complex mechanisms responsible for the reduction of metal cations. Ultimately, this would result in an improved control over the conversion of the ions into nanoparticles. This calls for further dedicated studies in order to achieve higher Pd(II) reduction yields. Nonetheless, for both gold and palladium, evidences point to a massive reduction of Au and Pd metal ions into NPs by a few minutes of plasma treatment only.

A good reconciliation of masses of metals contained in the NPs pellet, the supernatant, the cleaning solution and the precursor solutions was found for gold (< 10% variation) and tin (< 5% variation). However, data reconciliation for palladium proved to be more difficult (~ 30% variation). The standard deviation for elemental recovery of palladium (10% - 15%) is also much higher than for the elemental recovery of gold (2% - 10%) and tin (< 0.5%).

3.3 Physicochemical analysis of nanoparticles by XPS

For the Au NPs synthesized from Au + Sn solutions, XPS results reveal the presence of carbon (47.7%), nitrogen (21.6%), oxygen (9.1%) and gold (21.5%), and the absence of Sn and K (Table 3). The latter two were present in the precursor solution in the form of tin ions and potassium oxalate, and their absence confirms the selectivity of the plasma recovery process to certain types of metal ions, such as gold. Table 4 presents the atomic percentages of each bands that were identified in high-resolution XPS for the synthesized NPs.(Moulder and Chastain, 1992) The corresponding high-resolution spectra are presented in Fig. 6 for both samples. In high resolution spectra (Table 4 and Fig. 6), the main band of the Au4f7/2 peak is located at 84.37 eV (Au; 19.14%) and a secondary band is located at 86.63 eV (Au + Sn; 2.36%).(Moulder and Chastain, 1992) The secondary band could be attributed to the presence of an intermetallic between Au and Sn, despite the fact that Sn could not detected in the survey spectra.(Moulder and Chastain, 1992) This small contribution is in agreement with the presence of 1.22 to 1.70% of the initial amount of Sn in the precursor fluid, detected in MP-AES sediments for the Au NPs (Table 2).

The C1s peak evidenced for the Au NPs is divided into two bands, located at 284.76 eV (C-C, C-H; 44.12%) and 287.14 eV (C-N, C-O-H; 3.61%). The C-N bond could be attributed to a certain fraction

of cyanide, a residue from the electroless plating solution. For oxygen, a single band constitutes the O1s peak at 532.07 eV (C-O, 9.13%). The excess carbon (C-C bond) and oxygen (C-O bond) could be related to atmospheric contamination of the Au NPs, or to remaining additives originating from the plating solution (ascorbic acid: $C_6H_8O_6$, hydroquinone: $C_6H_8O_2$).

Although a fraction of the very significant nitrogen contribution could be related to the cyanide (CN^-) present in the precursor solutions, this peak cannot be attributed to aurocyanide complexes (e.g. $KAu(CN)_2$), since shifts on the Au4f7/2 peak corresponding to the $Au(CN)_2^-$ ion would correspond to 84.9 - 85.2.(Cook et al., 1989) In addition to this, the nitrogen contribution can only be partly attributed to CN^-, as the total %C attributed to C-N and C-O-H bonds is not more than 3.61% in total. Because of the relatively small contribution of O (9.13% in total), nitrogen does not seem to be attributed either to nitrite (NO_2^-) and nitrate ions (NO_3^-) that could be generated as a result of degradation of the CN^- ions by the UV photons. The high levels of nitrogen apparently not associated to either C nor O, are most probably associated with the presence of ammonium ions commonly used for pH adjustment in gold-containing plating bath solutions (e.g. with ammonium hydroxide, NH_4OH).(Azmah Hanim, 2017)

For the Pd NPs synthesized from Pd acetate solutions, the XPS results reveal the presence of carbon (40.4%), nitrogen (7.5%), oxygen (16.6%), phosphorus (6.6%), iodine (6.0%), silicon (2.9%) and palladium (20.1%). Phosphorus comes from the reducing agent hypophosphite, nitrogen from thiourea (stabilizer). Iodine is an additive to the precursor solution to accelerate metal deposition, whereas silicon is for the bare substrate on which the Pd NPs are deposited. The absence of sodium from the XPS spectrum could indicate that sodium hypophosphite ($NaPO_2H_2$), an additive used during the electroless plating process of Pd, was successfully discarded from the plasma-treated solution after centrifugation.

However, the presence of phosphorus suggests that the sodium hypophosphite was degraded during plasma treatment, in the form of phosphate or phosphonate.

In high-resolution spectra (Table 4, Fig. 6), the C1s peak is divided into two bands, located at 284.91 eV (C-C, C-H; 31.32 %) and 286.78 eV (C-N, C-O-H; 9.03%; from atmospheric contamination and from acetate). Thiourea (CH_4N_2S) could be responsible for the C-N contribution. Thiourea acts as a stabilizer for the Pd-based electroless plating solution used by the semiconductor industries. It also preserves the pH of the electroless baths. For oxygen, three bands could be extracted from the O1s peak. They can be found at 531.80 eV (C-O, 9.48%; mainly from atmospheric contamination and from acetate), 533.07 eV (N-O, 5.54%; possibly from NO_2^- or NO_3^- ions generated during the plasma process) and 534.61 eV (SiO_2, 1.55%; from the base substrate). Finally, the single contribution for Pd corresponds to the synthesized Pd NPs, and no evidence of oxidation was found.

Overall, the results suggest that the purification procedure successfully removed some of the impurities originating from the electroless plating effluents, such as tin, potassium and sodium. However, further steps would be necessary in order to completely remove the remaining contaminants (e.g. cyanide, hypophosphite degradation product, iodine, etc.), although the absence of ligands at the surface of the synthesized NPs could make them useful for applications in the catalyst industry.(Maye et al., 2003; Yang and Bao, 2017)

Table 3. Chemical composition of the Au and Pd NPs synthesized from the plating solutions, extracted from survey spectra obtained by XPS analyses.

Element	Atomic percentage [%] Au NPs (n = 3)	Atomic percentage [%] Pd NPs (n = 1)
C	47.7 ± 4.0	40.4
N	21.6 ± 4.4	7.5
O	9.1 ± 1.0	16.6
Au	21.5 ± 0.8	0.0
Sn	0.0 ± 0.0	0.0
Pd	0.0 ± 0.0	20.1
K	0.0 ± 0.0	0.0
Si	0.0 ± 0.0	2.9
P	0.0 ± 0.0	6.6
I	0.0 ± 0.0	6.0

Table 4. Atomic percentages determined from high-resolution XPS, for the Au and Pd NPs synthesized by plasma treatment.

Sample	Peak	Binding energy [eV]	Bond	Area [%]	Atomic percentage [%]
Au NPs (n = 3)	C1s	284.76	C-C, C-H	92.3 ± 2.4	44.1 ± 4.8
		287.14	C-N, C-O-H	7.7 ± 2.4	3.6 ± 0.9
	O1s	532.07	C-O	100.0 ± 0.0	9.1 ± 1.0
	Au4f7/2	84.37	Au	95.6 ± 1.7	20.5 ± 0.7
		86.63	Au + Sn	4.5 ± 1.7	0.96 ± 0.03
Pd NPs (n = 1)	C1s	284.91	C-C, C-H	77.6	31.3
		286.78	C-N, C-O-H	22.4	9.0
	O1s	531.80	C-O	57.2	9.5
		533.07	N-O	33.5	5.5
		534.61	SiO_2	9.4	1.6
	Pd3d5/2	335.63	Pd	100.0	20.1

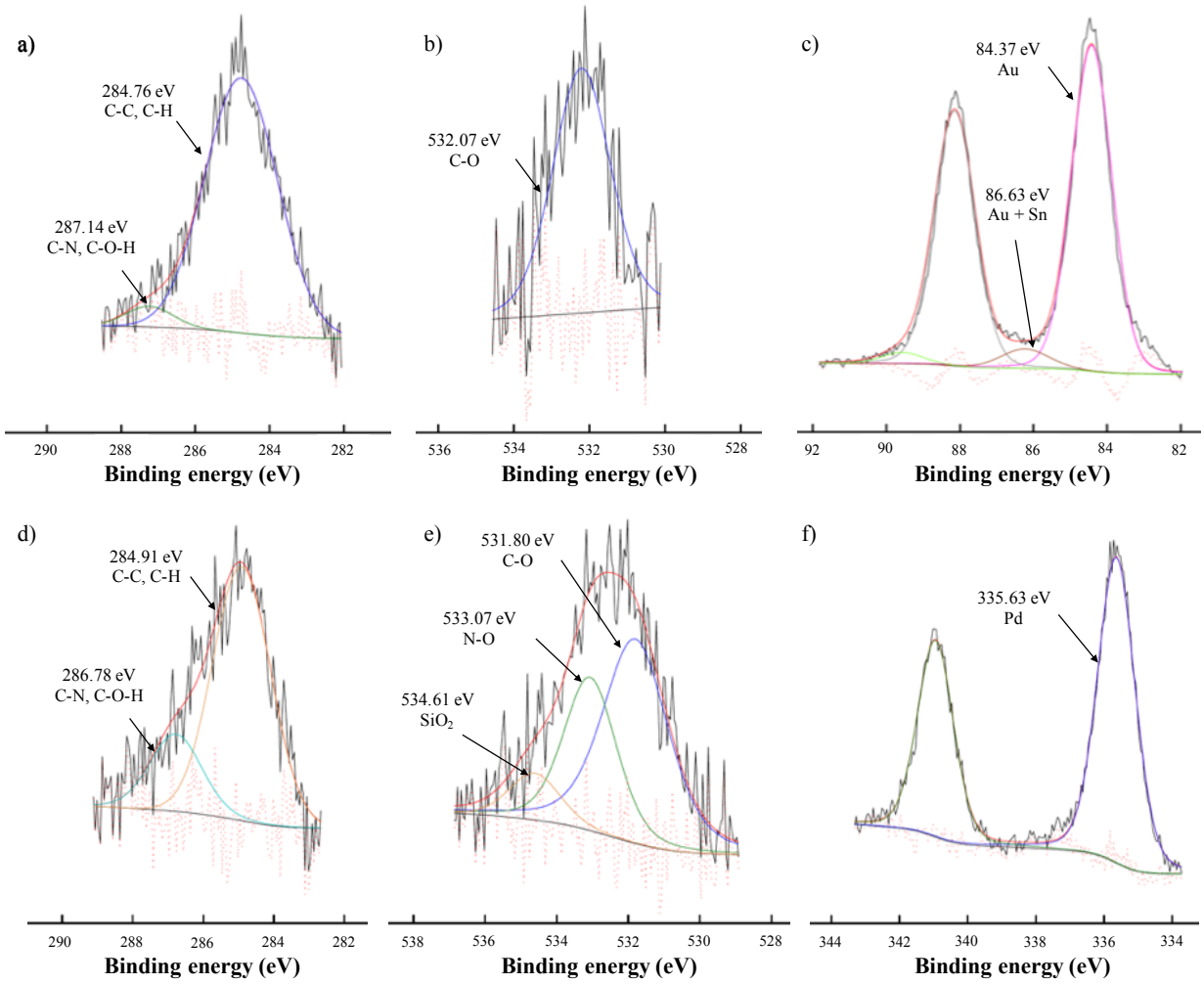

Fig. 6. High-resolution XPS spectra: Au NPs: a) C1s, b) O1s and c) Au4f; Pd NPs: d) C1s, e) O1s, f) Pd3d.

3.4 Size measurements (TEM, DLS)

Both types of NPs were analyzed by transmission electron microscopy (Fig. 7). The TEM images (Fig. 7 a, c) revealed a similar aspect for both types of NPs, spherical with some evidences of triangular forms. Nanoparticles were present in the form of large agglomerates, as expected for Pd and Au NPs in the absence of molecular surfactants. Isolated NPs were still observed for Au NPs, which could be due to strong electrostatic repulsion induced by the ammonium ions present at their surfaces. The mean

diameter of the synthesized Au NPs was 14.8 nm ± 3.0 nm. Unfortunately, strong agglomerations were found on the Pd NPs TEM grids and therefore no size distribution could be performed with this product.

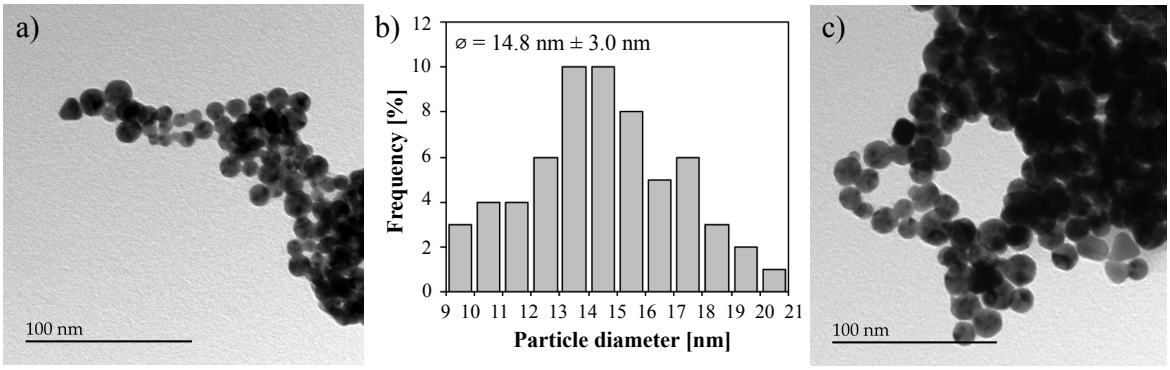

Fig. 7. a) TEM image of Au NPs synthesized by a 5-min plasma-treatment, b) corresponding size distribution (n = 300 particles), and c) TEM image of Pd NPs synthesized by a 5-min plasma-treatment.

DLS measurements were performed on all solutions (see in supporting information Fig. S1), which further confirmed the strong agglomeration state of the NPs. All the samples showed a polydispersity index greater than 0.2 (PDI > 0.2), which indicates that the plasma-treated solutions are not colloidally stable. This is in good agreement with the quick sedimentation of the particles that was observed after recovering the solutions from the plasma reactor. In just a few minutes, most of the synthesized particles were already accumulated at the bottom of their container. Rapid agglomeration and efficient sedimentation would be an advantage for the rapid recovery of the synthesized particles through e.g. centrifugation.

During the plasma process, the nucleation and growth of metal ions to nanoparticles depends on numerous parameters, such as the area of the treated solution, the type of plasma used in the DBD, the power of the discharge, the duration of the treatment, the pH of the solution, the presence of impurities, and the nature of the reactive species induced in solution by application of the plasma discharges.(Kortshagen et al., 2016; Lin and Wang, 2015; Mariotti and Sankaran, 2010; Ostrikov et al.,

2011) Recent studies have reported that the metastable reactive oxygen and nitrogen species (ROS and RNS) produced by the interaction of plasma discharges with the treated aqueous solutions could also be involved in the reduction of metal ions to nanoparticles.(Burlica et al., 2006; Hamaguchi, 2013; Kong et al., 2011; Mariotti and Sankaran, 2010; Nosenko et al., 2009; Yukinori et al., 2012) For instance, the generation of reducing agents such as hydrogen peroxide (H_2O_2), hydrogen radicals and hydroxyl radicals has been associated with the nucleation of metal nanoparticles during plasma treatment of aqueous solutions.(Saito et al., 2017)

In 2016, the finished semiconductor products market was estimated at 327 billion US$, and about 6% of this market involved the production of at least one electroless plating part.(IC Insights, 2018; Markets and Markets, 2016; Statista, 2017) On a yearly basis, this industry generates large volumes of discarded fluids that must be treated either by toxic cyanides (for Au recovery) or by using the long, relatively inefficient and largely non selective batch electrowinning process. Overall, the total metal content in the discarded solutions is estimated to 40 million US$ per year.(IC Insights, 2018; Markets and Markets, 2016; Statista, 2017) Therefore the plasma treatment technology could find advantageous niche applications to accelerate the recovery process of precious metals contained in plating effluents, while keeping the process greener (e.g. without cyanides). Gold and palladium recovered by electrowinning and by cyanidation are usually converted in “dore” bars and sold at a fraction of the gold and palladium value content to precious metal refiners.(Marsden and House, 2006) The present study indicates that Au and Pd NPs generated by the plasma process contain high elemental ratios in Au and Pd, respectively. In addition, the potential of these noble metal nanoparticles for catalytic applications could be explored and this would turn the produced NPs into a high-value industrial product. However, their use for applications in the catalyst industry would require further purification steps (e.g. additional

centrifugation steps, filtration through membranes, chemical and thermodynamic ligand removal steps, etc.), in order to decrease the percentages of oxygen and nitrogen observed in the XPS results, due to the presence organic ligands at the nanoparticle surfaces. These strategies abound in the literature of catalysis and in industrial practices in the field. They could be explored as an obvious next step. On the other hand, dore bars could also be produced by sedimentation and melting of nanoparticles, should the purification steps prove too costly for an economical production of high-purity nanoparticles for catalysis. The dore bars, a high-value intermediate product in the refining steps of gold for jewellery and banking fields, would still be of much higher purity and thus reach higher market values compared to conventional dore bars produced through cyanidation and electrowinning.(Marsden and House, 2006) Overall, a complete economic analysis of the plasma process and its following steps (purification, etc.) would be necessary in order to identify the optimal application for these NPs (catalyst industry after purification, or smelting into dore bars if the purification of the NPs proves to be too expensive).

A comprehensive comparative cost analysis between plasma technology, electrowinning and cyanidation would be difficult to realize at this step, since the plasma reactor used in this study is for laboratory use only (i.e. not optimized for pilot plant production). Moreover, the consumables and the equipment involved in each process differ. However, the ratio between the energy consumption of the plasma reactor and the recovered mass of gold and palladium, can be quickly estimated for both the plasma process and electrowinning. By considering a scenario in which all noble metals in the fluid would be recovered by plasma process in not more than 5 min (operating at 40 W), the total energy consumption of the plasma reactor would be 3.33 Wh, for an electrical energy consumption of 73 kWh/kg Au and 546 kWh/kg Pd produced, respectively. The electrical consumption ratio for electrowinning was estimated to 112 kWh/kg Au for dilute Au solutions (5 mg L^{-1} Au), and this for several hours of treatment.(Brandon et al., 1987) The energy consumptions of both technologies would be in the same

range, and possibly less expensive for plasma extraction, a much more rapid alternative to electrowinning. Plasma extraction does not require the use of cyanides, and the perspective of greener Au extraction processes is of considerable interest in the precious metal refining industry.(Marsden and House, 2006)

In the present study, a mixture of argon and hydrogen was used to ensure the recovery of noble metals by plasma treatment. From the economic standpoint, the consumption of argon can prove relatively costly, while the use of hydrogen needs to be well controlled in the industrial environment. Therefore, the possibility to use nitrogen or air plasma could further increase the interest towards the plasma extraction process, by significantly reducing operating costs and safety issues. Naturally, the elemental recovery of noble metals could be affected by the metastable species generated in solution, depending on the nature of the plasma discharges. Such aspects will be explored in dedicated studies.

Plasma-based recovery processes for noble metals could potentially be applied to different types of effluents, with varying compositions, metal concentrations and pH. In fact, previous work from our research group confirmed the possibility to synthesize Au NPs from synthetic solutions containing Au(III) ions at a low concentration of 0.1 mM, while achieving high reduction yields (99.81%).(Bouchard et al., 2017) Moreover, the results from this study demonstrated that Au NPs could be synthesized from low pH (< 0.5) precursor solutions, while achieving moderate reduction yields (56%). Therefore, gold ions present in various valence states (Au(I) or Au(II)), concentrations and under different pH conditions can be effectively reduced by species generated by the plasma discharges. Such promising results suggest the application of the DBD plasma recovery process to a variety of wastewaters and leachates.

4 Conclusion

This study demonstrates for the first time the possibility to extract precious metals (Au, Pd) from electrolyte baths used in the electroless plating process of the semiconductor industry, which produces very large volumes of discarded solutions on a yearly basis. An atmospheric plasma process reduces metal ions into Au and Pd NPs, which can be recovered by sedimentation and centrifugation. The process, much more rapid and efficient than electrowinning, was also found to be selective to the gold ions present in Au + Sn solutions. In fact, this study demonstrates for the first time the strong potential of plasma technology for the selective extraction of one precious metal ion (e.g. Au) from solutions that contain several metal ions species. The results suggest the possibility to replace cyanidation by plasma extraction process to enable the production of higher-purity and thus higher value dore bars that could be sold by the semiconductor foundries directly to precious metals refiners. The results from physicochemical and particle size analysis also suggests the possibility of integrating the as-synthesized NPs as a high-value product in e.g. catalysis technologies. Overall, the use of plasma technology could open several doors for new hydrometallurgy-based recycling processes in the semiconductor companies.

Funding

This work was supported by the Natural Sciences and Engineering Research Council of Canada [RGPIN-2017-06173].

CRediT authorship contribution statement

Jean-François Sauvageau: Conceptualization, Methodology, Validation, Formal analysis, Investigation, Data curation, Writing - original draft, Visualization. Marc-André Fortin: Conceptualization,

Methodology, Validation, Resources, Writing - review & editing, Supervision, Project administration, Funding acquisition.

Declaration of Competing of Interests

The authors declare that they have no known competing financial interests or personal relationships that could have appeared to influence the work reported in this paper.

Acknowledgements

The authors would like to thank an industrial partner for providing the waste solutions, as well as Mrs. Vicky Dodier (Université Laval) for her contribution to the MP-AES analyses, Mr. Richard Janvier (Université Laval) for his contribution to the TEM images, and Dr. Pascale Chevallier (Cr-CHU de Québec – Université Laval) for her contribution to XPS analyses.

Appendix A Supplementary data

Supplementary data to this article can be found online at https://doi.org/10.1016/j.hydromet.2020.105483.

References

Ali, I. et al., 2019. Overview of microbes based fabricated biogenic nanoparticles for water and wastewater treatment. J. Environ. Manag.., 230, 128-150. doi.org/10.1016/j.jenvman.2018.09.073.

Azmah Hanim, M.A., 2017. 3.15 Electroless plating as surface finishing in electronic packaging. In: Comprehensive Materials Finishing. Elsevier, Oxford, p. 10.

Barbosa, L., Sobral, L.G.S. and Dutra, A., 2001. Gold electrowinning from diluted cyanide liquors: performance evaluation of different reaction systems. Miner. Eng. 14 (9), 963-974. doi.org/10.1016/S0892-6875(01)00104-2.

Baudrand, D. and Bengston, J., 1995. Electroless plating processes: developing technologies for electroless nickel, palladium, and gold. Met. Finis. 93 (9), 55-57. doi.org/10.1016/0026-0576(95)99502-2.

Bednar, N., Matovic, J. and Stojanovic, G., 2013. Properties of surface dielectric barrier discharge plasma generator for fabrication of nanomaterials. J. Electrost. 71 (6), 1068-1075. doi.org/10.1016/j.elstat.2013.10.010.

Bouchard, M., Laprise-Pelletier, M., Turgeon, S. and Fortin, M.A., 2017. Efficient and rapid synthesis of radioactive gold nanoparticles by dielectric barrier discharge. Part. Part. Syst. Charact. 34 (2), 10. doi.org/10.1002/ppsc.201600231.

Bouchard, M., Létourneau, M., Sarra-Bournet, C. and Laprise-Pelletier, M., 2015. Rapid nucleation of iron oxide nanoclusters in aqueous solution by plasma electrochemistry. Langmuir 31, 7633−7643. doi.org/10.1021/acs.langmuir.5b01235.

Brandenburg, R., 2017. Dielectric barrier discharges: progress on plasma sources and on the understanding of regimes and single filaments. Plasma Sources Sci. Techno. 26 (5). doi.org/10.1088/1361-6595/aa6426.

Brandon, N., Mahmood, M., Page, P. and Roberts, C., 1987. The direct electrowinning of gold from dilute cyanide leach liquors. Hydrometallurgy 18 (3), 305-319. doi.org/10.1016/0304-386X(87)90072-7.

Burlica, R., Kirkpatrick, M.J. and Locke, B.R., 2006. Formation of reactive species in gliding arc discharges with liquid water. J. Electrost. 64 (1), 35-43. doi.org/10.1016/j.elstat.2004.12.007.

Cook, R., Crathorne, E.A., Monhemius, A.J. and Perry, D.L., 1989. An XPS study of the adsorption of gold (I) cyanide by carbons. Hydrometallurgy 22 (1), 171-182. doi.org/10.1016/0304-386X(89)90048-0.

C.R.C. Press, 2007. CRC Handbook of Chemistry and Physics: 88th ed. http://archive.wikiwix.com/cache/?url=http%3A%2F%2Fwww.hbcpnetbase.com%2F (accessed 25 February 2020)

Datta, M. and Osaka, T., 2005. Microelectronic Packaging. In: New Trends in Electrochemical Technology Series, 3, CRC Press LLC, p. 24-26.

Foster, J.E., 2017. Plasma-based water purification: challenges and prospects for the future. Phys. Plasmas 24 (5), 055501. doi.org/10.1063/1.4977921.

Frost, K., Hua, I. and Ieee, 2017. A spatially explicit assessment of water use by the global semiconductor industry. 2017 IEEE Conference on Technologies for Sustainability. IEEE, New York, p. 4.

Hamaguchi, S., 2013. Chemically reactive species in liquids generated by atmospheric-pressure plasmas and their roles in plasma medicine. AIP Conf. Proc, 1545 (1), 214-222. doi.org/10.1063/1.4815857.

Hijosa-Valsero, M., Molina, R., Schikora, H., Muller, M. and Bayona, J.M., 2013a. Removal of cyanide from water by means of plasma discharge technology. Water Res. 47 (4), 1701-1707. doi.org/10.1016/j.watres.2013.01.001.

Hijosa-Valsero, M., Molina, R., Schikora, H., Muller, M. and Bayona, J.M., 2013b. Removal of priority pollutants from water by means of dielectric barrier discharge atmospheric plasma. J. Hazard. Mater. 262, 664-673. doi.org/10.1016/j.jhazmat.2013.09.022.

IC Insights, 2018. Global Wafer Capacity. http://www.icinsights.com/services/global-wafer-capacity (accessed 25 February 2020)

Kim, H.S. et al., 2013. Use of plasma gliding arc discharges on the inactivation of E-Coli in water. Sep. Purif. Technol. 120, 423-428. doi.org/10.1016/j.seppur.2013.09.041.

Kogelschatz, U., 2003. Dielectric-barrier discharges: their history, discharge physics, and industrial applications. Plasma Chem. Plasma Process 23 (1), 1-46. doi.org/10.1023/a:1022470901385.

Kogelschatz, U., 2007. Applications of microplasmas and microreactor technology. Contrib. Plasma Phys. 47 (1-2), 80-88. doi.org/10.1002/ctpp.200710012.

Kogelschatz, U., Eliasson, B. and Egli, W., 1999. From ozone generators to flat television screens: history and future potential of dielectric-barrier discharges. Pure Appl. Chem. 71 (10), 1819-1828. doi.org/10.1351/pac199971101819.

Kong, M.G., Keidar, M. and Ostrikov, K., 2011. Plasmas meet nanoparticles-where synergies can advance the frontier of medicine. J. Phys. D-Appl. Phys. 44 (17), 14. doi.org/10.1088/0022-3727/44/17/174018.

Koo, I.G., Lee, M.S., Shim, J.H. and Lee, W.M., 2005. Platinum nanoparticles prepared by a plasma-chemical reduction method. J. Mater. Chem. 15, 4125–4128. doi.org/10.1039/B508420B.

Kortshagen, U.R. et al., 2016. Nonthermal plasma synthesis of nanocrystals: fundamental principles, materials, and applications. Chem.l Rev. 116 (18), 11061-11127. doi.org/10.1021/acs.chemrev.6b00039.

Lee, S.W., Janyasupab, M., Liu, C.C. and Sankaran, R.M., 2013. Fabrication of Ir nanoparticle-based biosensors by plasma electrochemical reduction for enzyme-free detection of hydrogen peroxide. Catal. Today 211, 137-142. doi.org/10.1016/j.cattod.2013.03.023.

Lin, L.L. and Wang, Q., 2015. Microplasma: a new generation of technology for functional nanomaterial synthesis. Plasma Chem. Plasma Process. 35 (6), 925-962. doi.org/10.1007/s11090-015-9640-y.

Loto, C.A., 2016. Electroless nickel plating - a review. Silicon 8 (2), 177-186. doi.org/10.1007/s12633-015-9367-7.

Luangpipat, T., Beattie, I.R., Chisti, Y. and Haverkamp, R.G., 2011. Gold nanoparticles produced in a microalga. J. Nanopart. Res. 13 (12), 6439-6445. doi.org/10.1007/s11051-011-0397-9.

Mariotti, D. and Sankaran, R.M., 2010. Microplasmas for nanomaterials synthesis. J. Phys. D-Appl. Phys. 43 (32), 21. doi.org/10.1088/0022-3727/43/32/323001.

Markets and Markets, 2016. Flip Chip Technology Market by Wafer Bumping Process (CU Pillar, Lead-Free), Packaging Technology (2D IC, 2.5D IC, 3D IC), Packaging Type (BGA, PGA, LGA, SIP, CSP), Product (Memory, LED, CPU, GPU, SOC), Application and Geography - Global Forecast to 2022. https://www.marketsandmarkets.com/Market-Reports/flip-chip-technology-market-264572064.html (accessed 25 February 2020)

Marsden, J. and House, I., 2006. The chemistry of gold extraction (2nd edition) John O Marsden and C Iain House SME. Gold Bull. 39 (3), 138-138. doi:10.1007/bf03215543.

Maye, M.M. et al., 2003. X-ray photoelectron spectroscopic study of the activation of molecularly-linked gold nanoparticle catalysts. Langmuir 19 (1), 125-131. doi.org/10.1021/la0264116.

McKenna, J. et al., 2011. Synthesis and surface engineering of nanomaterials by atmospheric-pressure microplasmas. Eur. Phys. J.-Appl. Phys 56 (2), 10. doi.org/10.1051/epjap/2011110203.

Moulder, J.F. and Chastain, J., 1992. Handbook of X-ray Photoelectron Spectroscopy: A Reference Book of Standard Spectra for Identification and Interpretation of XPS Data. Physical Electronics Division, Perkin-Elmer Corporation, p. 260.

Nosenko, T. et al., 2009. Low-temperature atmospheric-pressure plasmas as a source of reactive oxygen and nitrogen species for chronic wound disinfection. Free Radic. Biol. Med. 47, S128-S128. doi.org/10.1016/j.freeradbiomed.2009.10.017.

Osaka, T., Okinaka, Y., Sasano, J. and Kato, M., 2006. Development of new electrolytic and electroless gold plating processes for electronics applications. Sci. Technol. Adv. Mater. 7 (5), 425-437. doi.org/10.1016/j.stam.2006.05.003.

Ostrikov, K., Cvelbar, U. and Murphy, A.B., 2011. Plasma nanoscience: setting directions, tackling grand challenges. J. Phys. D-Appl. Phys. 44 (17), 29. doi.org/10.1088/0022-3727/44/17/174001.

Richmonds, C. and Sankaran, R.M., 2008. Plasma-liquid electrochemistry: rapid synthesis of colloidal metal nanoparticles by microplasma reduction of aqueous cations. Appl. Phys. Lett. 93 (13), 3. doi.org/10.1063/1.2988283.

Saito, N., Bratescu, M.A. and Hashimi, K., 2017. Solution plasma: a new reaction field for nanomaterials synthesis. Jpn. J. App. Phys. 57 (1), 0102A4. doi.org/10.7567/JJAP.57.0102A4.

Sauvageau, J.F., Turgeon, S., Chevallier, P. and Fortin, M.A., 2018. Colloidal suspensions of platinum group metal nanoparticles (Pt, Pd, Rh) synthesized by dielectric barrier discharge plasma (DBD). Part. Part. Syst. Charact. 35 (4), doi.org/10.1002/ppsc.201700365.

Shacham-Diamand, Y., Osaka, T., Okinaka, Y., Sugiyama, A. and Dubin, V., 2015. 30 years of electroless plating for semiconductor and polymer micro-systems. Microelectron. Eng. 132, 35-45. doi.org/10.1016/j.mee.2014.09.003.

Statista, 2017. Distribution of global gold demand by industry in 2017. https://www.statista.com/statistics/299609/gold-demand-by-industry-sector-share/, 2017. (accessed 25 February 2020)

Vorobyova, T.N., Poznyak, S.K., Rimskaya, A.A. and Vrublevskaya, O.N., 2004. Electroless gold plating from a hypophosphite-dicyanoaurate bath. Surf. Coat. Technol. 176 (3), 327-336. doi.org/10.1016/s0257-8972(03)00744-8.

Wang, R.X. et al., 2015. Microplasma-assisted synthesis of colloidal gold nanoparticles and their use in the detection of cardiac troponin I (cTn-I). Plasma Process. Polym. 12 (4), 380-391. doi.org/10.1002/ppap.201400127.

Xu, W.Y. et al., 2012. Low-temperature plasma-assisted preparation of graphene supported palladium nanoparticles with high hydrodesulfurization activity. J. Mater. Chem. 22 (29), 14363-14368. doi.org/10.1039/c2jm16479e.

Yang, P. and Bao, Y.S., 2017. Palladium nanoparticles supported on organofunctionalized kaolin as an efficient heterogeneous catalyst for directed C-H functionalization of arylpyrazoles. RSC Adv. 7 (85), 53878-53886. doi.org/10.1039/c7ra11800g.

Yukinori, S., David, B.G., Hung-Wen, C., Tetsuji, S. and Gregor, E.M., 2012. Plasma chemistry model of surface microdischarge in humid air and dynamics of reactive neutral species. J. Phys. D. Appl. Phys. 45 (42), 425201. doi.org/10.1088/0022-3727/45/42/425201.

Supporting Information

Recovery of Noble Metal Elements from Effluents of the Semiconductor Industry as Nanoparticles, by Dielectric Barrier Discharge (DBD) Plasma Treatment

*Jean-François Sauvageau and Marc-André Fortin**

In addition to the TEM studies, DLS analyses were performed on both NPs suspensions in order to determine their hydrodynamic diameter. Immediately after completion of the plasma treatments, aliquots from the solutions were collected for DLS measurements. **Figure S1** shows the DLS spectra that were acquired for both types of NPs suspensions. The DLS results clearly show polydispersity and aggregation for both the Au NPs and Pd NP suspensions, which is expected since no surfactant was used in this study to provide either electrostatic or steric hindrance between the particles.

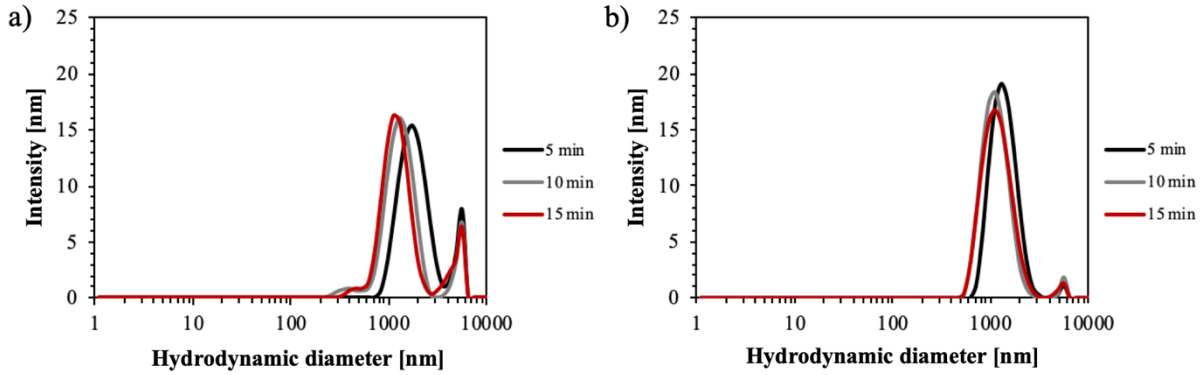

Fig. S1. DLS spectra in intensity for a) Au NPs suspensions and b) Pd NPs suspensions. Both spectra are indicative only, as PdI confirm broad particle size distributions, with evidences of agglomerations.